Reviewer comments in black, author replies in green.

Reviewer 1:

I believe that the authors have done a great job revising the manuscript. I have only a couple of technical comments below.

1. P. 3 L. 21: The equation is mathematically incorrect. If an error term is included on the right-hand side, then the appropriate error terms have to be included on the left-hand side too.
We have included the error terms on the left.

2. P. 5 L. 12: in simulate O2 fields → in simulated O2 fields
Changed.

3. P. 8 L. 32: 2O flux → O2 flux
This was corrected to N2O flux.

Reviewer 2:

This paper includes some valuable calculations and the authors have made some good progress toward clarifying their methodology. However, some of the methodological details remain difficult to follow. It also appears that the authors have used only a small subset of the available pN2O data in MEMENTO, for reasons that aren't clear. This subset appears to have a summertime bias in the South Atlantic and a wintertime bias in the North Atlantic. Since pN2O is the one of the main constraints used in the model optimization, these seasonal biases may affect the results.
Please see our point-by-point reply below.

I support publication of this paper in principle, but before it is ready I still think there are a number of details that should be clarified and sections of text that could be written more clearly.
Specific comments

p2L32. The text here mentions 4 methods. Are these 4 enumerated in the lines that follow? For example, is the following method 1,"We extend the global ocean biogeochemistry model PlankTOM10 with additional N cycle processes."? Or are these additional approaches (it seems like there are more than 4 total)? Please start the sentences with transition words like, "First", "Second" instead of just "We" to make this clear. Is the sentence on line35 starting with "Then" approach # 3? If so, please use "Third" This is a key paragraph where the authors lay out what the paper will do, yet I am already lost.
We do not mention 4 methods, but "4 observational databases". These databases are presented in Section 2.2, where they are enumerated ((1), (2), (3), (4)). We have clarified the text from p2L32 onwards, to link the modifications of the model to these four databases. We hope this clarifies our methodology.

P3L30/P4L1. There are a lot more deep and surface N2O data in MEMENTO than the reported n=8047 and n=6136 mentioned here. Were only a subset of the available data selected and why? Also, were the surface data generally in units of ppb and the deep data in nmol/L?

We have used all the data available in the MEMENTO database (on the download dates mentioned) for our analysis. Line 26 states "The number of datapoints reported for each database are after gridding to 1°× 1°× 12 months × 33 depths (World Ocean Atlas 2009)." It is true that the MEMENTO database contains more individual measurements, but these are often taken at high spatial and/or temporal resolution, that do not provide additional constraints on the results. We have added the original number of data points.
We have added units to the description of the 4 databases.

P4L4 Are deep data converted to delta_pN2O or just the surface data? If deep data are converted too, please mention that this necessitates first converting the deep nM data to ppb using a solubility function. This is a large uncertainty. The statement "we have taken the database at face value" is inadequate for conveying the extent of the uncertainties involved in combining nM and ppb data in equation 3.
We did not convert deep data to delta_pN2O, as the analyses involving measurements in ppb (i.e., air-sea flux estimation in section 3.2) is conducted separately from those involving the deep data in nM (i.e., the analyses constraining N2O production in low O2 regions in Section 3.1). We have clarified this at the end of the introduction and it is repeated in Sections 3.1 and 3.2. See also the next question.

P.4 Section 2.4 (Nitrification) and p5 Section 2.5 (NH4+ uptake) appear to be databases 1 and 2 of the 4 mentioned. I was expecting 2.6 then to be MEMENTO deep N2O and 2.7 to be MEMENTO surface data. Instead, we jump to 2.6 N2O production. This is an example of why it remains challenging to follow the methodology of this paper.
We have clarified which database is used in which section, stating at the end of the introduction that database (1) is used in Section 2.4, database (2) in Section 2.5, database (3) in Section 3.1 and database (4) in Section 3.2. This is because databases (1) and (2) are used for model development while databases (3) and (4) are used for constraining the N2O budget.

P4L27. Does Yool provide an actual data base, or simply assume a constant rate of 0.2 /day everywhere (as written, the sentence implies the latter)?
Both. Yool provided the database of nitrification rate which we use in our analysis. In the same paper, Yool also published model results where they use a constant rate of 0.2/day which we use as the departure point for our analysis. We clarified the text in section 2.4.

Section 2.4. Given that a cost function of 2 means that, on average, the model deviates from the observations by a factor 2 (Section 2.3), does this paragraph suggest that the model deviates from observations by a factor of > 4 on average? In other words, it provides no real constraint. Shouldn't that be stated explicitly somewhere in this section? Is there any meaningful difference between a cost function of 4.22 and 4.16?
Indeed a cost function of >4 is not very satisfactory, though it is not unusual when confronting model results with noisy databases, such as those of ecosystem variables. We modified the text to stress that the differences between 4.22 and 4.16 are minimal. We acknowledge the weak constraints of this database in multiple places in our manuscript. In Section 2.4, by using such phrases "observed nitrification rates are highly variable", "poorly constrains the temperature dependence of AOA" , "a slightly improved representation of the observations" , "which limits the range of O2 concentrations" , "reflecting a lack of data to parameterise an expected decrease" , "this estimate is not well constrained". The weak constraints of the data are further stressed in the Discussion: "This lack of data synthesis and of identification of the most important controls in a complex system is reflected in a relatively low ability of the model to model observed nitrification rates", and "This lack of

knowledge also means that partitioning the global marine N2O production over the nitrification and denitrification pathways is poorly constrained". Finally, we recognised further the weak constraint by omitting our estimate of the low O2 N2O production from the abstract.

P5L34. So, the diagnostic model dN2O/AOU ratios are not optimized against the MEMENTO database using the cost function? The intro and the mention of the 4 datasets had led me to expect they would be.
This is indeed ambiguous. We have added an explanation and clarification to the text: "Previous studies using regional databases have found different oxic ratios (Suntharalingam and Sarmiento 2000 and references therein). Therefore, both the oxic and hypoxic ratios have been reoptimised to the global databases (Sect. 3.1 - 3.2)."

P6L11-12 "We indenpendently optimised the ratios of N2O production and consumption from denitrification" These are minor terms in the budget compared to N2O production from nitrification. Why wasn't that ratio/coefficient optimized?
Both databases were used to optimise separate parameters. To clarify this, P6L14 was rewritten: "The low O2 ratios of both submodels (supplementary material Section 8.7) were optimised using the database of observed N2O concentration (Sect. 3.1) and the oxic ratios of both submodels were optimised using the database of observed DeltapN2O (Sect. 3.2)".

P6L14 "The ratios of both submodels were optimized using the databases of observed N2O concentration and pN2O" Is this referring to the deep N2O or the surface N2O data or both?
Both databases were used to optimise separate parameters. To clarify this, it was rewritten: "The low O2 ratios of both submodels (supplementary material Section 8.7) were optimised using the database of observed N2O concentration (Sect. 3.1) and the oxic ratios of both submodels were optimised using the database of observed DeltapN2O (Sect. 3.2)".

Figure 3 caption. Please specify where these values are from (model, MEMENTO, etc).
Section 2.1 states: "The globally averaged ΔN2O/AOU ratio was calculated from the MEMENTO database (Bange et al., 2009) as 81.5 ± 1.4 μmol/mol (Fig. 3)". This information was moved from the caption to the main body of the text at the previous request of this reviewer (reviewer 2, L72).

Figure 3 annotation shows 0.0815 + 2.7551, but this is reported on p3L15 as 81.5 ± 1.4 μmol/mol. First, the error has completely changed. Second, there is a switch from nmol N2O and umol AOU in the figure to units of umol/mol in the text, with a factor of 1000 thrown in to add to the confusion. Better to be consistent across figure and text.
The annotation shows slope and intercept (0.0815x + 2.7551), not the standard deviation of the slope. The units in the text were changed to have mol rather than μmol in the denominator following the previous request of this reviewer (reviewer 2, L262). We note that changing the axes in Fig. 3 to mol O2 and μmol N2O would make the numbers on the axes run from -0.0003 to 0.0004 and -0.00005 to 0.0002 and therefore difficult to read.

Figure 6/Section 2.5. The model is credited with reproducing "the large scale pattern of surface NH+4 concentration (which) shows an increase with latitude." However, the performance seems pretty poor and the pattern could equally well be described as high in the Southern Ocean (where nutrient utilization is known to be low) and around continental boundaries where there is nutrient input from land. Similar to Section 2.4, the cost function of 3 seems quite large and suggests there's no real constraint here.

The description of the uncertainty was toned down at the previous request of this reviewer (reviewer 2, L144). The text immediately preceding that quoted by the reviewer here still acknowledged the highly variable individual observations and the shortcomings in the model. We have rephrased the latter to clarify it: "the model produces a much smoother distribution of NH4 concentrations than the observations". Our statement on the large-scale patterns was motivated by the comparisons demonstrated in Fig. 6, in particular the zonal average in Fig. 6C, which show an increase with latitude in both hemispheres.

Figure 9 and 11 caption and Equation 5 on p. 6. What does MSE stand for? Please spell it out in all these places. (The captions should be understandable without referring back to the text.)
We have added to Section 2.8 after Eq. 5 that: "MSE is mean square error:"

Section 2.8 Should Equation 6 be presented before 5? It seems like 5 builds upon the definition of MSE introduced in Eq 6.
In Eq. 2 and 4 we use the same order of presentation as in Eq. 5, with the equation stating what we want to calculate first, followed by clarifications of the form "in which …".

P7L26. I'm confused by the use of "even though" here. Given that the prognostic model represents N2O consumption in the OMZ, why would that be expected to improve (i.e., increase) the concentration of N2O between 200 and 1500m?
This was clarified to: "even though the prognostic model is more detailed, separately representing the processes of N2O production and consumption at low O2 concentrations.".

P8L5-7. These sentences belong in the methodology. Also, as mentioned above, why isn't the nitrification N2O/NO3 ratio optimized too? That seems like the most important term in the model.
This was moved to the methodology. We clarified p6L14: "the oxic ratios of both submodels were optimised using the database of observed DeltapN2O (Sect. 3.2)". Section 3.2 states: "In the prognostic model, the optimised oxic nitrification ratio was 123 µmol N2O (mol NH4+)".

P8L14 I would suggest writing as 0.183 mmol N2O, to avoid switching units, which is confusing for the reader.
We have used the unit of µmol N2O here to enable consistency with our discussion in the following section (3.2).

P8L16-17. "pN2O provided a better constraint than the N2O concentration distribution" Back in Section 2.2, deep N2O is mentioned as dataset number 3 used to optimize the fluxes. The sentence just cited suggests that deep N2O is not actually used. Please clarify.
Both databases were used to optimise separate parameters. To clarify this, P6L14 was rewritten: "The low O2 ratios of both submodels (supplementary material Section 8.7) were optimised using the database of observed N2O concentration (Sect. 3.1) and the oxic ratios of both submodels were optimised using the database of observed DeltapN2O (Sect. 3.2)".

Figure 10a) This figure represents only 6136 data points (I think there are a factor of 10 more surface N2O data in MEMENTO than that), yet the figure suggests extensive coverage of the global ocean, and near complete coverage in the Atlantic. Have the data been binned and gridded and if so how? It seems like a single data point has been expanded as a ~5x5 pixel, which implies much better coverage than may really exist. Also, what is the seasonal distribution of the data? I suspect the South Atlantic data are all from austral summer, while

the North Atlantic data are mainly from fall/winter. I don't think the Atlantic is undersaturated to the extent implied by this figure on an annual basis. Can the data be binned by season and plotted in a 4 panel plot?

For gridding see P3L26. We added to the Fig.6 and 10 legend that "observations (symbol size is 5 × 5°)".

The model was subsampled in the same months as the observations, so any seasonal sampling bias in the observations would be reproduced in the model. Because of this, and because the paper already has 12 figures, we have not included the seasonal distribution in the paper, but reproduce it below, showing that (1) no, South Atlantic data is not limited to austral summer, (2) no, North Atlantic data are not limited to fall/winter, but (3) yes, the undersaturation in the North Atlantic is mostly limited to fall (there is no data North of 4°N in the North Atlantic in winter).

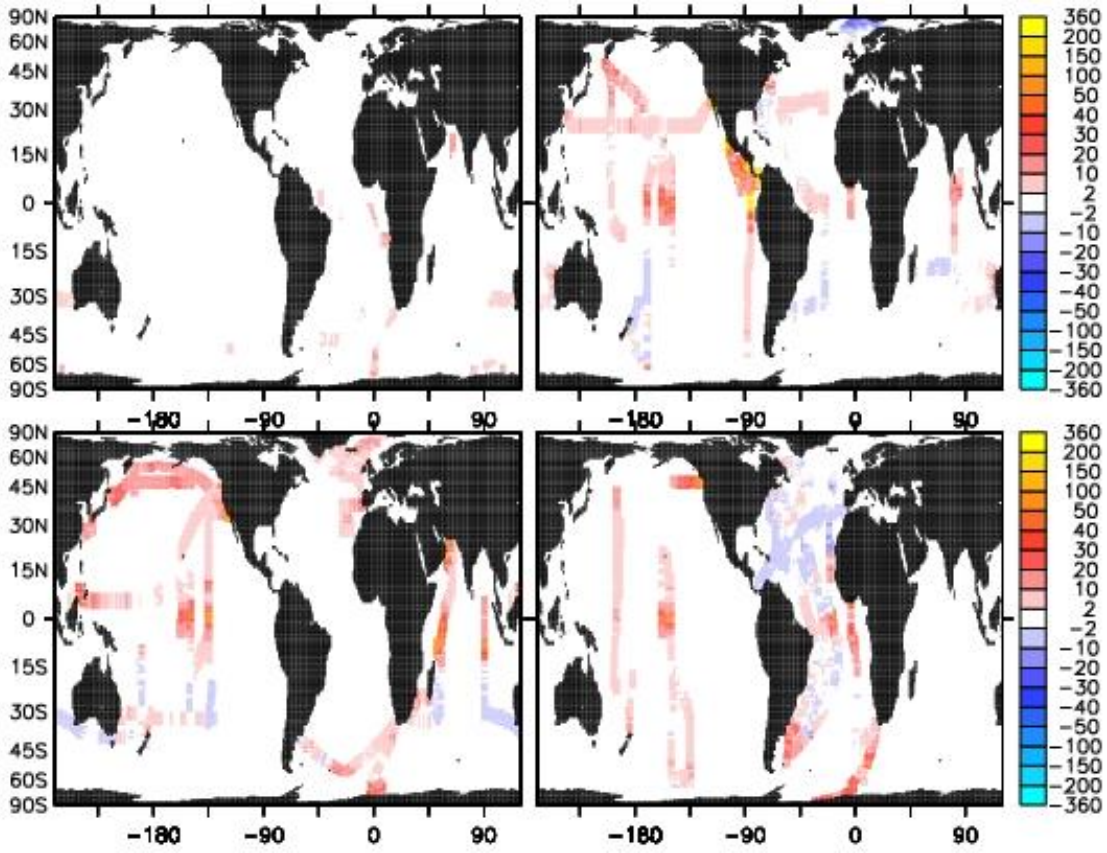

Upper left DJF, upper right MAM, lower left JJA, lower right SON.

Figure 10b) Following on the above comment, it is confusing to plot the "same months where there are observations, and annual averages everywhere else," especially if there are strong seasonal biases that differ by region. I would again suggest 4 panel seasonal plot for the model results.

By plotting the model in the same months where there are observations, if the model seasonal sampling is biased relative to the annual average this become visible as a colour contrast between the sampled and unsampled areas. We are analysing a global flux, so seasonal and spatial details are relevant only to the extent that they define the uncertainty interval around the central global N2O flux estimate. Because the piston velocity, rather than model-data differences are the biggest source of uncertainty, we did not include these additional figures in the main text. The seasonal model figures are included below.

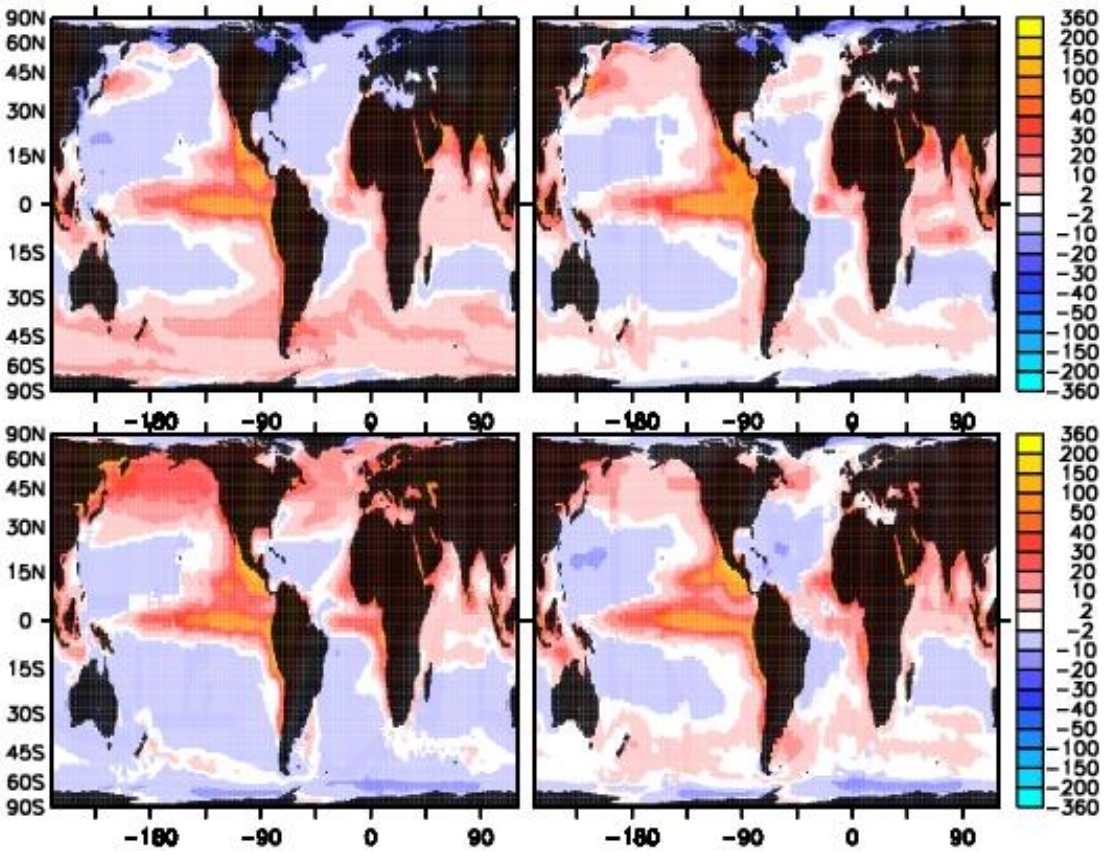

Diagnostic model, seasons in same panels as observations.

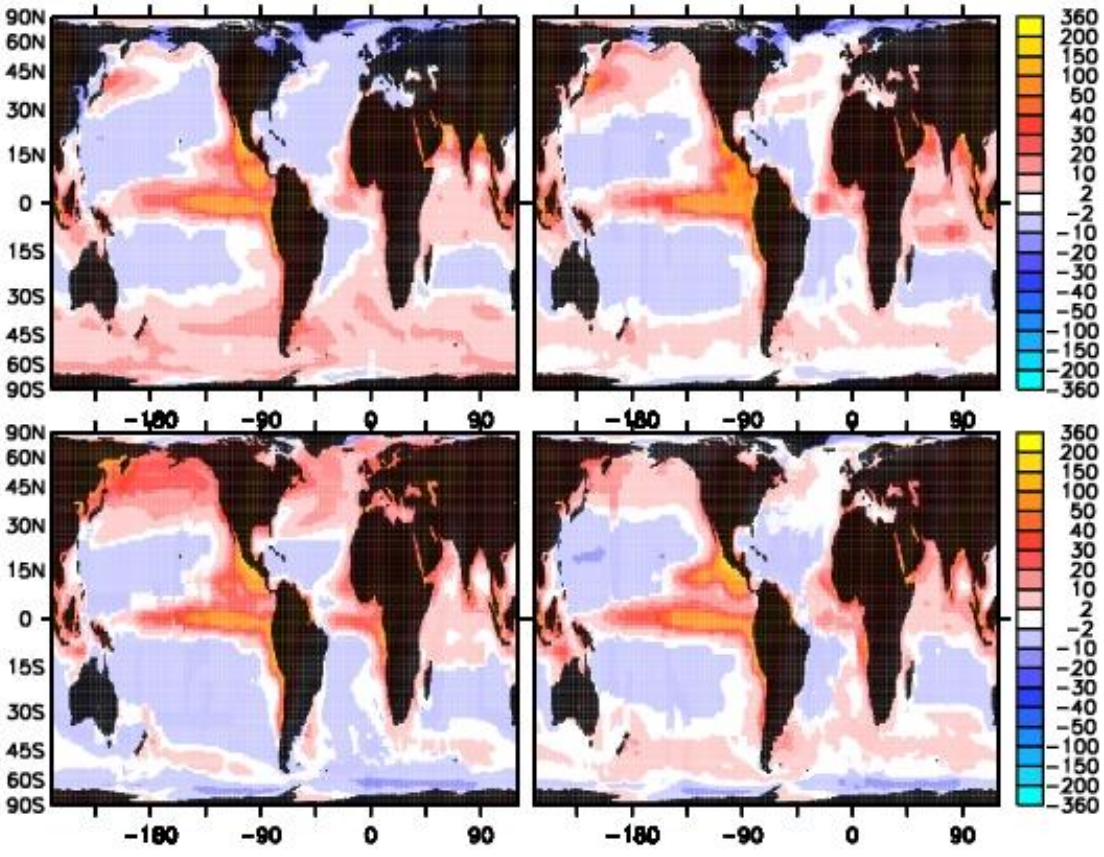

Prognostic model, seasons in same panels as observations.

Figure 10b) Also, the red contours appear to smear over the black continents.
This may be due to the 9-fold compression that Latex performs between the figure .eps and the .pdf. If the editor wishes, we can provide the original .eps.

Figure 10d) Please make green and red lines thicker. They are illegible.
Done.

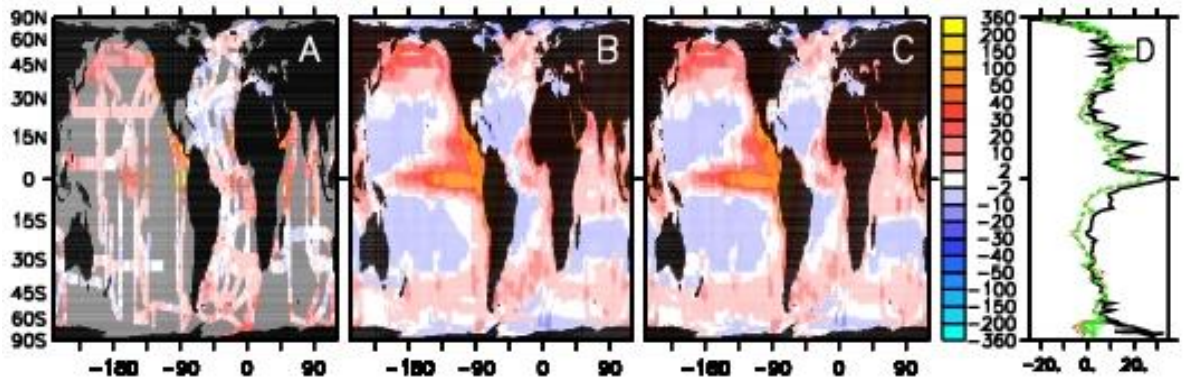

Figure 11. Are the different symbols (0.06, 0.11, 0.17, 0.34 for A) and (0.07, 0.12, 0.17, 0.34 for B) essentially the same thing or is the similarity in numbers pure coincidence? If the former, why the slight differences (e.g., 0.06 v. 0.07) and inconsistent shapes? Also, why does A say "different symbols indicate different low O2 ratios" while B says "points with the same symbols have different N2O ratios for nitrification." I thought the nitrification ratio was not optimized.
The numbers are different because A) is the diagnostic model and B) is the prognostic model, but they are similar because the optimised low O2 N2O production rates and their confidence intervals are similar in the two submodels, so the perturbations we chose around the optima were also similar.
The different terminology in the panel A and panel B legends reflects the different representations of N2O production/consumption in the diagnostic model and the prognostic model, respectively.
In fact, Figure 11 shows the optimisation of the nitrification ratio. For more details on how we clarified that the nitrification ratio is being optimised see our answers to P6L11-12 and P6L14.

P8L23-24. This implies that the oxic nitrification ratio is optimized, at least in the prognostic model. Yet as far as I can tell, the Methods only describe optimizing the denitrification and suboxic N2O parameters.
Yes, the oxic nitrification rate was optimised for both models.
Both databases were used to optimise separate parameters. To clarify this, P6L14 was rewritten: "The low O2 ratios of both submodels (supplementary material Section 8.7) were optimised using the database of observed N2O concentration (Sect. 3.1) and the oxic ratios of both submodels were optimised using the database of observed DeltapN2O (Sect. 3.2)".

P8L23 and L32. Are deep offshore and near-shore non-coastal synonymous? Please use consistent terminology to avoid confusion.
Yes, they are the same. Deep offshore was replaced by near-shore non-coastal throughout.

P9L8 Again, it is important to know whether the surface pN2O data used were originally in ppb units or in nM. If the latter, these measurements likely have an uncertainty of +/- 0.5 nM

or more, such that the 3% cited here (which may be accurate for the solubility function per se) greatly understates the actually uncertainty in ppb due to the solubility conversion.
We added the units (ppb) in Section 2.2.

P9L19-20 “In light of this, we decided to recalculate the N-cycle-based N2O production based on currently available data. We find that we can estimate all the relevant steps in the N cycle with observational data” These seem like non sequiturs. The logic here is difficult to follow.
We have rewritten this to make it more clear, by replacing
“Suntharalingam et al. (2012) note that N2O production is proportional to export production. However, this is dependent on the model formulation, which was based on earlier studies that suggested nitrification in the ocean surface layer was light-inhibited (e.g. Horrigan et al. 1981). More recent analyses of nitrification, e.g. the database of Yool et al. (2007), find widespread nitrification in the upper mixed layer. In light of this, we decided to recalculate the N-cycle-based N2O production based on currently available data. We find that we can estimate all the relevant steps in the N cycle with observational data, including their uncertainty (Sect. 2.1). At present this uncertainty, at 4.6 ± 3.1 Tg N y −1 . The biggest contributor to this uncertainty”
with
“We use an updated estimate of primary production and it's error (Buitenhuis et al. 2013), and compile a database of the f-ratio (Fig. 2). We also use a much larger database of the DeltaN2O/AOU ratio (Fig. 3). We recalculate the N-cycle-based N2O production based on these extended databases. We find that we can estimate all the relevant steps in the N cycle with observational data, including their uncertainty (Sect. 2.1). At present this uncertainty is still fairly large , at 4.6 ± 3.1 Tg N y−1. The uncertainty in this estimate is similar to that in Cohen and Gordon (1979), but our uncertainty is based on the uncertainty in all components of the calculation, while their uncertainty was based only on the uncertainty in the DeltaN2O/AOU ratio. The upper 60% of our estimate overlaps with the lower 62% of the Cohen and Gordon (1979) estimate. The biggest contributor to our uncertainty”.

P9L26 NO3- is the electron ACCEPTOR in denitrification. Organic C is the electron donor.
Apologies. This was corrected.

P9L28. “this estimate” Better to restate the numbers, e.g., 4.6 +/- 3.1 vs. 2.5 +/- 0.8. More importantly, these two errors are estimated in very different ways, such that it is not clear they are directly comparable. The authors are comparing a global back-of-the-envelope calculation, with large global errors on any given parameter, to a more grid-specific calculation. Of course the latter will have smaller uncertainty.
We have restated the numbers.
The error in the N-cycle calculation is dominated by the uncertainty in the f-ratio. If that uncertainty could be brought down to the second highest relative error of 12%, the uncertainty would be reduced to 1 Tg N y-1. We have added that: “additional measurements and/or data-synthesis could help constrain the N2O budget.”.

P9L30. Please use “further” only once in this sentence and perhaps break into 2 sentences.
The second further was replaced by extend.

P9L30 What does “their” refer to?
We replaced “their model representation” with “the model representation of these N cycle processes”.

Discussion section in general. The writing and organization of thoughts could use improvement. Please avoid starting sentences with “This” unless the antecedent is clear.

The only time when “This” is not accompanied by a noun that specifies the antecedent (“This NO3”, “This lack of data”, etc.) is on P10L34. We replaced “This” by “This constraint” and added “so that the integrated total can be well constrained even if the individual processes are not”.

Constraints on global oceanic emissions of N_2O from observations and models

Erik T. Buitenhuis[1,2], Parvadha Suntharalingam[1], and Corinne Le Quéré[1,2]

[1]School of Environmental Sciences, University of East Anglia, Norwich, United Kingdom
[2]Tyndall Centre for Climate Change Research, University of East Anglia, Norwich, United Kingdom

Correspondence to: Erik T. Buitenhuis (E-mail: http://greenocean-data.uea.ac.uk/.feedback.html)

Abstract. We estimate the global ocean N_2O flux to the atmosphere and its confidence interval using a statistical method based on model perturbation simulations and their fit to a database of ΔpN_2O (n=6136). We evaluate two submodels of N_2O production. The first submodel splits N_2O production into oxic and hypoxic pathways following previous publications. The second submodel explicitly represents the redox transformations of N that lead to N_2O production (nitrification and hypoxic denitrification) and N_2O consumption (suboxic denitrification), and is presented here for the first time. We perturb both submodels by modifying the key parameters of the N_2O cycling pathways (nitrification rates, NH_4^+ uptake, N_2O yields under oxic, hypoxic and suboxic conditions), and determine a set of optimal model parameters by minimisation of a cost function against 4 databases of N cycle observations derived from observed and model ΔpN_2O concentrations. Our estimate of the global oceanic N_2O flux resulting from this cost function minimisation is 2.4 $\pm$ 0.8 and 2.5 $\pm$ 0.8 Tg N y^{-1} for the 2 N_2O submodels. These estimates suggest that the currently available observational data of surface ΔpN_2O constrain the global N_2O flux to a narrower range relative to the large range of results presented in the latest IPCC report.

1 Introduction

Nitrous oxide (N_2O) is the third most important contributor to anthropogenic radiative forcing, after carbon dioxide (CO_2) and methane (CH_4) (**?**). It is also currently estimated as the dominant contributor to stratospheric ozone depletion (**?**). Yet our quantitative understanding of the magnitude and processes controlling natural N_2O emissions from the Earth surface to the atmosphere is very poor. A range of methods have been used to constrain total oceanic N_2O emissions, including the combination of surface ocean N_2O partial pressure anomalies with gas-exchange parameterizations (**?**), empirically derived functional relationships applied to global ocean datasets (**??**), and ocean biogeochemistry models (**????**). In spite of the multiple methods used, the reported oceanic emissions of N_2O is still poorly constrained, ranging from 1.9 to 9.4 Tg N y^{-1} according to the latest report of the Intergovernmental Panel on Climate Change (IPCC **?**). The uncertainty in the oceanic emissions of N_2O accounts for a large part of the total uncertainty in the natural N_2O emissions, which are approximately 11 Tg N y^{-1} (**?**). Part of the uncertainty in the oceanic emissions is whether estuaries are included, which could emit as much as 2.3 - 3.6 Tg N y^{-1} (**?**).

The large uncertainty in the oceanic emissions of N_2O stems from the complexity of its production pathways. There are two main pathways of N_2O production in the ocean, nitrification and denitrification, which both stem from redox reactions of nitrogen, under oxic and hypoxic conditions, respectively (Fig. 1). N_2O is formed as a byproduct of marine nitrification of ammonium (NH_4^+) to nitrate (NO_3^-); N_2O is also an intermediate product of denitrification, during the reduction of NO_3^- to nitrogen gas (N_2) (**???**). Denitrification can also consume N_2O, using extracellular N_2O, and reduce it to N_2 (**?**). In the oxic part of the ocean (i.e. most of the ocean, 97% >34 μmol O_2 L^{-1} (using O_2 data taken from **?**)) denitrification is suppressed, and the primary formation pathway is usually ascribed to nitrification (**?**), although denitrification may be significant in the anaerobic centres of large marine snow particles in oxic waters (**?**). Oceanic N_2O production in oxic regions is often derived from the linear relationships observed between apparent oxygen utilization (AOU) and apparent N_2O production (ΔN_2O) (e.g. **??**). However, the ΔN_2O/AOU ratio varies in different water masses and oceanic regions (**?**). Previous studies have suggested that differences in the ΔN_2O/AOU ratio could be driven by changing N_2O yields under varying pressure and temperature (**?**) or varying O_2 concentration (**?**). Additional mechanisms not yet quantified could include variations in the elemental stoichiometry of the organic matter that is being remineralised, and spatial separation of organic matter remineralisation and nitrification. Throughout the manuscript we will refer to N_2O stoichiometries relative to O_2, NH_4^+ and NO_3^- as ratios, because they have been optimised against global databases of concentration measurements, rather than from microbiological yields. Using the latter would be more mechanistically satisfying, but the relevant yields are at present insufficiently constrained by observations.

Estimates of the contribution from suboxic regions of the ocean (about 3%) to the global N_2O flux vary from net depletion via denitrification (**?**), to 33% for the total N_2O production in the suboxic ocean (**?**), and to more than 50% from denitrification alone (**?**). This ambiguity remains unresolved. Bottom-up microbial physiology data is relatively scarce (see ~~Sect.~~ Sections 2.4 - 2.6), while top-down data needs relatively complicated inverse methods to estimate the contribution from suboxic regions. These inverse methods are complicated both because of the variation in the ΔN_2O/AOU ratio, which is negative under suboxic conditions, maximal under hypoxic conditions and lower under oxic conditions (e.g. 0.31 - 0.033 mmol/mol, **?**), and because the influence of mixing gradients make in situ ratios an unreliable gauge to the biological yields under in situ conditions (**?**).

Here, we estimate the global ocean N_2O flux to the atmosphere and its confidence interval. First, we estimate N_2O flux from observations only (Sect. 2.1). This estimate has large uncertainty. We subsequently use a statistical approach introduced by **?** to estimate the global oceanic emissions of N_2O and its confidence interval by combining ocean N_2O model simulations with a global database of measurements of surface ΔpN_2O. This approach involves minimisation of a cost function that compares a series of model simulations with a global database of point measurements of surface ΔpN_2O. To achieve this, we use 4 observational databases of the N cycle (Sect. 2.2)~~to~~. We extend the global ocean biogeochemistry model PlankTOM10 (**?**) with additional N cycle processes. We derive the biogeochemical parameters for nitrification rate and phytoplankton use of NH_4^+ from the observational databases of nitrification rate and NH_4^+ concentration (~~databases (1) and (2) and Sect. 2.4-2.5~~Sect. 2.3-2.4). Then, we describe two separate submodels of different levels of complexity that represent N_2O cycling pathways (Sect. ~~2.6~~2.5-2.7). Finally, we apply the statistical approach ~~(Sect. 2.8)~~ to the two submodels to estimate the N_2O production in the low O_2 regions from the depth resolved N_2O concentration database (~~database (3) and Sect.~~ Section 3.1), and the global

oceanic N_2O flux from the surface ΔpN_2O database (~~database (4) and Sect.~~ Section 3.2), followed by a discussion of the results (Sect. 4).

2 Ocean N cycle

2.1 Calculation of global ocean N_2O production from N cycle observations

In this section we provide an initial estimate of global marine N_2O production based on observationally derived quantities characterising marine productivity and the global ocean N cycle. This follows a similar method to **?**, who estimated ocean N_2O production using Redfield type ratios. N_2O is produced either during production of NO_3^- in NH_4^+ oxidation or during NO_3^- reduction in denitrification (Fig. 1). We therefore base the N_2O production on total NO_3^- turnover, calculated from primary production times the f-ratio. The f-ratio is the fraction of primary production that is supported by nitrate. Primary production (PP) was estimated at 58 $\pm$ 7 Pg C y^{-1} based on ^{14}C primary production measurements (n=50,050), parameter perturbations of a previous version of the model uses here, and Eq. 5 (**?**). We compiled a database of uptake rates of NO_3^-, NH_4^+ and urea, which gives an average f-ratio of 0.29 $\pm$ 0.18 (Fig. 2, large symbols, n=34). The globally averaged ΔN_2O/AOU ratio was calculated from the MEMENTO database (**?**) as 81.5 $\pm$ 1.4 μmol/mol (Fig. 3). Finally, since primary production is expressed in carbon terms, and N_2O production was correlated with oxygen (O_2) utilization, we need to include the -O_2:C ratio (the - sign indicates the O_2 is consumed as CO_2 is produced), which was taken from **?** as 170 $\pm$ 10 / 117 $\pm$ 14, and the molar weights of C (12) and N in N_2O (28). Here and in the rest of the paper, errors were progagated in the usual way:

$$error = \sqrt{(\frac{errorofA}{A})^2 + (\frac{errorofB}{B})^2 + ... * A * B * ...} \quad (1)$$

Thus N_2O production was calculated as PP *f-ratio*-O_2:C *ΔN_2O/AOU. Our best estimate of N_2O production using this method is 58 ~~$\pm$ 7~~ *1000 ~~*0.29 $\pm$ 0.18 *170 $\pm$ 10~~ * 0.29 * 170/117 ~~$\pm$ 14 *81.5e-6 $\pm$ 1.4~~* 81.5e-6 *28/12 = 4.6 $\pm$ 3.1 Tg N y^{-1}. This estimate lies in the middle of other reported estimates (Fig. 4) but the 68% confidence interval is very large. We therefore investigate the N_2O fluxes using a model ~~optimised~~ optimized with observations in the rest of the paper.

2.2 Observational databases for model development

We used four databases to tune or optimise different aspects of the N cycle in the PlankTOM10 ocean biogeochemistry model. The number of datapoints reported for each database are after gridding to 1°$\times$ 1°$\times$ 12 months $\times$ 33 depths (World Ocean Atlas 2009). The databases used are (1) NH_4^+ specific nitrification rate (~~d^{-1}, raw data n=425, gridded data~~ n=296) as described in Yool et al. (2007); (2) surface NH_4^+ concentration distribution (~~μmol L^{-1}, raw data n=33079, gridded data~~ n=2343) that combines the dataset used in **?** with data held by the British Oceanographic Data Centre in January 2014 (Johnson et al. in prep., http://www.bodc.ac.uk); (3) depth-resolved N_2O concentration from the MEMENTO project ~~(nmol L^{-1}, https://memento.geomar.de/; **?**, ; e~~ and (4) surface partial pressure of N_2O (pN_2O) also from MEMENTO (~~ppb,~~ n=6136; downloaded 16 Sept. 2015~~, raw data n=227463, gridded data n=6136~~). Since there is at present no formal quality control beyond that performed by individual contributors to the MEMENTO database and a check by the database administrators that the values make physical sense (**?**), we

have taken the database at face value. pN_2O was converted to ΔpN_2O using atmospheric pN_2O:

$$pN_2O_{atm} = 0.000009471353 \times Y^3 - 0.052147139 \times Y^2 + 95.68066 \times Y - 58228.41 \quad (2)$$

(A. Freing, pers. comm., correction to **?**), in which Y is the decimal year. The average absolute difference relative to the global average pN_2O_{atm} data from the NOAA/ESRL Global Monitoring Division (ftp://ftp.cmdl.noaa.gov/hats/n2o/combined/HATS_global_N2O.txt) is 0.5 ppb between 1977 and 2014 and 0.3 ppb between 2000 and 2014.

2.3 Cost Function Formulation

To parameterise the model N cycle, we use a cost function to minimize the difference between model and observations, following the methods of **?**:

$$costfunction = 10^{\Sigma|log_{10}(model/observation)|/n} \quad (3)$$

This formulation gives equal weight to the relative correspondence between model and observations at small and large observational values. A value of 2 means that, on average, the model deviates from the observations by a factor 2 in either direction. To calculate the cost function (and also to calculate MSE in Eq. 6), the model was regridded to the same grid as the observations, and residuals were calculated at months and places where there are observations. The cost function results for the optimised simulations are summarised in Table 1.

2.4 Nitrification

Our initial biogeochemical model configuration is PlankTOM10 (**?**), which represents growth and loss terms from ten Plankton Functional Types (PFTs), including N_2-fixers, picoheterotrophs (*Bacteria* plus *Archaea*) and denitrification rate, but not denitrifier biomass. A full model description and parameter values are provided in the supplementary material. Here, we extend the model representation of redox reactions in the N cycle, to create the global biogeochemical model PlankTOM10.2. We describe the new N cycle components below.

In order to represent nitrification rate, the state variable for dissolved inorganic nitrogen was split into NO_3^- and NH_4^+. Respiration by all PFTs produces NH_4^+. The parameterization for nitrification used in our model is based on the analysis of a database of NH_4^+-specific nitrification rates (**?**). **?** found that observed nitrification rates are highly variable, with no obvious relationship with either latitude or depth. ~~In their model they~~ They therefore used a constant rate of 0.2 d^{-1} throughout the ocean in their model. Implementing this rate in our model resulted in a cost function relative to the nitrification rate observations of 4.22 (Table 1). We tested if including temperature, O_2 or light dependence improves the ability of the model to reproduce observed nitrification rates. Regarding the response of ammonia oxidizing *Archaea* (AOA), the main nitrifiers in the ocean (**???**), to temperature, we are only aware of the measurements of **?**. These show a ~4-fold variation in maximum growth rate between 3 strains, which poorly constrains the temperature dependence of AOA. We therefore first used a generic Q_{10} of 2 and optimised the rate at 0°C using the nitrification rate observations. This led to ~~only~~ a slightly improved representation of the observations (cost function = 4.18). Although the response of AOA and ammonia oxidizing *Bacteria* (AOB) to O_2 has only

been measured at 21-25 °C (**??**), which limits the range of O_2 concentrations, there was a significant logarithmic relationship between N_2O yield and O_2 (Fig. 5). A logarithmic function fit the data better than linear, exponential or power functions. Since nitrification consumes O_2, in the model it decreases as remineralisation switches from O_2 to NO_3 (supplementary material Eq. 70, 61, 67). Implementing this response to O_2 led to ~~only~~ a further small improvement of the model nitrification rate relative to the observations (cost=4.16). This implies that nitrification never becomes O_2 limited, reflecting a lack of data to parameterise an expected decrease. As will be described more fully in ~~Sect.~~ Section 3.1, we used observed O_2 concentrations in the simulations (**?**) rather than interactively modelled O_2, to minimise the impact of model biases in ~~simulated~~ simulate O_2 fields (**?**). The response of AOA to light is estimated to be 50% inhibited at 5 μmol photons m^{-2} s^{-1}. However, this estimate is not well constrained (**?**). Implementing this light response did not improve the model, either in combination with the O_2 and temperature responses or with the temperature response only, and was subsequently omitted. The lack of improvement in nitrification rates by adding light inhibition might reflect the lower sensitivity of AOA to light found by **?**.

2.5 Phytoplankton $K_{1/2}$ for NH_4^+ uptake

We used the calculation of the preferential uptake of NH_4^+ over NO_3^- by phytoplankton PFTs of **?**(supplementary material Eq. 9). The $K_{1/2}$ of phytoplankton for NH_4^+ has mostly been measured based on uptake rates (syntheses by **??**). **?** have shown a theoretical expectation of a linear increase of $K_{1/2}$ with cell radius. The observations are so variable that they neither confirm nor contradict such an increase. The model uses a fixed C:N:O_2 ratio for all organic matter of 122:16:-172, and Michaelis-Menten kinetics for growth based on inorganic N uptake by phytoplankton (**?**, supplementary material Eq. 8, 9). We therefore need a $K_{1/2}$ for growth rather than for uptake to be consistent with the fixed C:N ratio (**?**). The available uptake rate data do not include the supporting data to allow conversion to the $K_{1/2}$ for growth. We are only aware of measurements of the $K_{1/2}$ for growth by **?**. Based on the latter values of 0.09 ± 0.15 μmol L^{-1} for picoeukaryotes, the $K_{1/2}$ of phytoplankton for NH_4^+ was set to 0.1 to 5 μmol L^{-1}, increasing linearly with nominal size (**?**). Due to the highly dynamic nature of NH_4^+ turnover, the ~~model produces a much smoother distribution of~~ ability of the model to reproduce the observed NH_4^+ concentrations ~~than the observations~~at the same times and places was by no means perfect, but the large scale pattern of surface NH_4^+ concentration shows an increase with latitude, consistent with the observations (Fig. 6), which translates into a cost function of 3.0.

2.6 N_2O production

N_2O production is implemented as two distinct submodels. The diagnostic submodel is based on statistical relationships of ΔN_2O/AOU ratios taken from observations and has previously been published (**??**). In oxic waters it uses one ratio to estimate the open ocean source of N_2O production. In hypoxic waters it uses a higher ratio to represent the increased yield of N_2O from both nitrification and denitrification in oxygen minimum zones. The hypoxic N_2O yield is maximal at 1 μmol O_2 L^{-1}, and decreases with an e-folding concentration of 10 μmol O_2 L^{-1} (**??**, supplementary material Eq. 69, 35, 67). ~~Previous studies using regional databases have found different oxic ratios (?, and references therein) . Therefore, both the oxic and hypoxic ratios have been reoptimised to the global databases (Sect. 3.1 - 3.2).~~

The prognostic submodel presented here is based on process understanding and explicitly represents the primary N_2O formation and consumption pathways associated with the marine nitrogen cycle (Fig. 1). It includes the production of N_2O during oxic nitrification (blue arrows in Fig. 1) and during hypoxic denitrification (red arrow in Fig. 1); and a consumption term during denitrification at even lower (suboxic) O_2 concentrations (yellow arrow in Fig. 1). The ratios of the three processes are globally invariant (supplementary material Eq. 70, 61, 63, 71). The functional form of the O_2 dependence of N_2O consumption (suppl. Eq. 71) was the same as that of denitrification (suppl. Eq. 67), and with an O_2 response function that is 1.5 μmol L^{-1} lower than that of denitrification, which is similar to that used by **?**. We indenpendently optimised the ratios of N2O production and consumption from denitrification (~~Sect.~~ Section 3.1), which controls the net N2O production as a function of O_2 concentration. There is not enough information at present to optimise the O_2 concentration parameters of denitrification and N_2O consumption as well. The ~~low O_2~~ ratios of both submodels ~~(supplementary material Section 8.7) were optimised using the database~~ were optimized using the databases of observed N_2O concentration ~~(Sect. 3.1) and the oxic ratios of both submodels were optimised using the database of observed~~ and ΔpN_2O (~~Sect.~~ see Sect. 3.1 and 3.2, supplementary material Section 8.7). The N2O concentrations from both the diagnostic and the prognostic submodels are transported in the same way by physical transport and the formulation of their gas exchange is also identical.

2.7 N_2O flux and simulation setup

N_2O is transported like other tracers. N_2O flux (=air-sea gas exchange) is calculated as:

$$N_2Oflux = (pN_2O_{atm} * K0 * (1 - p_{watervapor}) - pN_2O) * piston\_velocity * \sqrt{660/Schmidt\_number_{N_2O}} * (1 - ice\_cover) \quad (4)$$

, in which K0 is the solubility (**?**), $p_{watervapor}$ is the water vapor pressure (**?**), piston velocity = 0.27*(wind speed)^2 (**?**), which is optimised for use with the NCEP reanalysis data used here, the Schmidt number for N_2O was taken from **?**, and the ice cover is calculated by the sea ice model LIM2.

In most of the simulations, atmospheric pN_2O was calculated from Eq. 2. For the optimised low O_2 production we also ran a series of simulations with the NOAA pN_2O_{atm} observational data that included seasonal and latitudinal variations (see ~~Sect.~~ Section 2.2 for the ftp address where we downloaded the data, and ~~Sect.~~ Section 3.2 for the results). Between 2000 and 2014, we used the monthly observations for the 12 available latitudes. Monthly anomalies relative to the global average were calculated at each available latitude from the 2000-2016 observations. These were added to Eq. 2 from 1965 and 1976, and to the global average observations between 1977 and 1999. In the model simulation, the data were linearly interpolated between the 12 latitudes and monthly observations.

The PlankTOM10.2 biogeochemical model coupled with the two N_2O submodels is incorporated into the ocean general circulation model NEMO v3.1 (**?**). The model resolution is 2° in longitude, on average 1.1° in latitude and has 30 vertical layers, from 10 m in the top 100 m to 500 m at 5000 m. The model simulations were initialised in 1965 from observations (**?**), with NH_4^+ initialised as 0, and N_2O initialised from a horizontal interpolation of the MEMENTO observations (see Sect.

2.2). Simulations were run to 2014, forced with daily atmospheric conditions from the NCEP reanalysis (**?**), (for details see **?**). Results are reported averaged over the last 5 years.

2.8 Estimation of global N_2O flux from point measurements of ΔpN_2O

In previous versions of the PlankTOM model (**???**) we have used Eq. 3 to evaluate the model because it minimises relative error, which we have found to be more appropriate when the observations span several orders of magnitude. Unfortunately, statistical confidence intervals have only been defined for χ^2-statistics such as Eq. 5 and 6, which minimise absolute error, so that we end up with 2 cost functions (Eq. 3, 5), depending on the application. To estimate the global air-sea flux of N_2O that best fits the ΔpN_2O data, and its $\pm$1-sigma (68%) confidence interval, we use the formula described in **?**:

$$MSE/MSE_{min} = 0.468 \times n/(n-2) \times \sqrt{(2(2n-2)/(n(n-4))) + n/(n-2)} \quad (5)$$

, in which ~~MSE is mean square error:~~

$$MSE = \frac{\Sigma(model(longitude, latitude, month) - observation(longitude, latitude, month))^2}{n} \quad (6)$$

, MSE_{min} is the MSE of the model simulation that is closest to the observations, and n is the number of ~~gridded~~ observations.

~~In addition to the uncertainty that arises from the model-observations mismatch, uncertainty is contributed by the uncertainties in the N_2O solubility and the piston velocity, the two quantities that connect the measured ΔpN_2O to the estimated air-sea flux. The uncertainty in the solubility has been estimated as 3(**?**) . The uncertainty in the piston velocity has been estimated at 32(**?**) . Uncertainties in the solubility and piston velocity are proportional to uncertainty in the optimised N_2O air-sea exchange because the optimised N_2O production needs to change proportionally with solubility and piston velocity to achieve the same ΔpN_2O.~~

3 Results

3.1 N_2O production at low O_2

The global N_2O production rate in oxygen minimum zones (OMZs) was ~~optimised~~ optimized using the depth-resolved N_2O data of the MEMENTO database. As noted in previous model studies of ocean O_2, global models do not well represent the extent and intensity of OMZ regions (**??**). The modeled OMZs in PlankTOM10 occur at greater depths than observed, resulting in unrealistic vertical distributions of N_2O (results not shown). Therefore, following **?**, the model was run using fixed observed O_2 concentrations (**?**), which corrected, in part, the vertical distribution of N_2O production from the two submodels, though it still occurred at too great depths (Fig. 7). In the equatorial regions and in the Pacific ocean the N_2O concentrations are underestimated between ~200 and ~1500 m. depth, and overestimated below that. This shortcoming is not significantly improved in the prognostic model (Fig. 7), even though the prognostic model ~~is more detailed, separately representing the processes~~ represents the process of N_2O ~~production and~~ consumption at low O_2 concentrations. The depth of maximum N_2O in

the model is generally deeper than observed, suggesting that organic matter remineralisation may be too low at shallow depths. This is confirmed by the depth profile of NO_3^-, which is underestimated relative to the WOA2009 observations between 100 and 1500 m., and overestimated at greater depths (Fig. 8). In both submodels, the N_2O concentrations in the deep sea are also too high, but since only 5% of N_2O production occurs below 1600 m this does not have a big impact on the global N_2O fluxes. The addition of N_2O consumption in the prognostic N_2O model does result in improvement of the N_2O depth profiles in the Indian Ocean.

In order to find the optimal N_2O production that minimizes the MSE (Eq. 5), we ran a range of simulations in which the low O_2 N_2O production was varied in the diagnostic model (Fig. 9A), and a range of simulations in which both the hypoxic N_2O production and the suboxic N_2O consumption were varied in the prognostic model (Fig. 9B). The optimum solution for the prognostic model was found at a gross production of 0.33 Tg N y^{-1}. The optimised (net) N_2O production in low O_2 regions and its confidence interval were 0.16 $\pm$ 0.13 Tg N y^{-1} for the diagnostic model, and 0.12 $\pm$ 0.07 Tg N y^{-1} for the prognostic model. In the ~~optimised~~ optimized diagnostic model the hypoxic N_2O ratio (i.e. net production) is 1.7 mmol N_2O (mol O_2)$^{-1}$. In the ~~optimised~~ optimized prognostic model the maximum N_2O production ratio (i.e. gross production from hypoxic denitrification) is 15.4 mmol N_2O (mol NO_3^-)$^{-1}$ decreasing to 0 above 34 μmol O_2 L^{-1}. The maximum N_2O consumption ratio (from suboxic denitrification) is 15 mmol N_2O (mol NO_3^-)$^{-1}$, decreasing to 0 above 28 μmol O_2 L^{-1}. This leads to net production that is always positive and has a maximal ratio of 183 μmol N_2O (mol NO_3^-)$^{-1}$ at 10 μmol O_2 L^{-1}.

3.2 N_2O flux

We used the surface ΔpN_2O distribution to constrain the total global N_2O flux~~, and the uncertainty arising from the model-data mismatch (the uncertainties arising from solubility and piston velocity are added at the end)~~. ΔpN_2O provided a better constraint than the N_2O concentration distribution, since more N_2O production mostly leads to more N_2O outgassing to the atmosphere rather than a significant increase in shallow N_2O concentrations (data not shown). This is because outgassing is proportional to ΔpN_2O, but N_2O concentration is proportional to pN_2O, and $\Delta pN_2O/pN_2O$ is small in most of the surface ocean. The zonal average surface ΔpN_2O distribution was well simulated by both submodels (Fig. 10D), and the model ensemble covered a wide range of global N_2O fluxes (Fig. 11). The total N_2O flux that best reproduced the ΔpN_2O distribution was 2.4 $\pm$ 0.3 Tg N y^{-1} for the diagnostic sub-model and 2.5 $\pm$ 0.3 Tg N y^{-1} for the prognostic sub-model (Fig. 11). In the diagnostic model, the ~~optimised~~ optimized oxic ΔN_2O/AOU ratio was 10.6 μmol N_2O (mol O_2)$^{-1}$. In the prognostic model, the ~~optimised~~ optimized oxic nitrification ratio was 123 μmol N_2O (mol NH_4^+)$^{-1}$. The results were the same in both diagnostic and prognostic submodels for the 2000-2004 and 2005-2009 averages, showing that the model was sufficiently spun up.

High N_2O fluxes have been reported for the coastal ocean (**?**) ~~, and~~ near-shore upwelling regions (e.g. **?**). To test whether these regions contribute more to the global N_2O flux than their surface area would suggest, we did the optimisation separately for the coastal ocean ($\leq$200 m bottom depth) for the near-shore non-coastal ocean ($\leq 2^\circ$ from land, >200m bottom depth) for the East Tropical Pacific (180° - 70°W, 5°S - 5°N, >2° from land), and the rest of the open ocean (Table 2). The results show that the coastal ocean contributes only 2% of the global N_2O flux, less than would be expected from its surface area, although there are also fewer observations in the coast (2% of the total) so that the relative error is slightly higher. The ~~near-shore~~

non-coastal deep offshore ocean contributes 14% of the global N_2O flux both submodels, hardly more than its areal percentage (13%), and it's also fairly well sampled (12% of the observations). The East Equatorial Pacific ocean contributes 27% in the diagnostic submodel and 25% in the prognostic model, more than its areal percentage (22%), and it's undersampled (17%). The open ocean contributes 57 - 59%, slightly less than its areal percentage (61%). This is as expected, because we've separated out the main N_2O hotspots, but the differences are quite small.

When we used observed atmospheric pN_2O that varied with latitude and month (see Sect. Section 2.2) the results were essentially the same, with an N_2O flux of 2.4 $\pm$ 0.3 Tg N y^{-1} for the diagnostic sub-model and 2.6 $\pm$ 0.3 Tg N y^{-1} for the prognostic sub-model (data not shown).

Finally, we add In addition to the uncertainty that arises from the model-observations mismatch, uncertainty is contributed by the uncertainties in the N_2O solubility and the piston velocity to the total , the two quantities that connect the measured ΔpN_2O to the estimated air-sea flux. The uncertainty in the solubility has been estimated as 3% (**?**) . The uncertainty in the piston velocity has been estimated at 32% (**?**) . Uncertainties in the solubility and piston velocity are proportional to uncertainty in the optimized N_2O flux through error propagation. This air-sea exchange because the optimized N_2O production needs to change proportionally with solubility and piston velocity to achieve the same ΔpN_2O. Through error propagation, this gives a total uncertainty of 2.4 $\pm$ 0.8 Tg N y^{-1} for the diagnostic sub-model and 2.5 $\pm$ 0.8 Tg N y^{-1} for the prognostic sub-model.

4 Discussion

? estimated global N_2O production directly from N cycle N-cycle observations. However, they did not have information on the f-ratio, so their estimate was based on total N assimilation in primary production. We use an updated estimate of primary production and it's error **?** , and compile a database of the f-ratio (Fig. 2).We also use a much larger database of the ΔN**?** note that N_2O/AOU ratio (Fig. 3). We O production is proportional to export production. However, this is dependent on the model formulation, which was based on earlier studies that suggested nitrification in the ocean surface layer was light-inhibited (e.g. **?**) . More recent analyses of nitrification, e.g. the database of **?** , find widespread nitrification in the upper mixed layer. In light of this, we decided to recalculate the N-cycle-based N_2O production based on these extended databasescurrently available data. We find that we can estimate all the relevant steps in the N cycle with observational data, including their uncertainty (Sect. 2.1). At present this uncertainty is still fairly large, at 4.6 $\pm$ 3.1 Tg N y^{-1}. The uncertainty in this estimate is similar to that in **?** , but our uncertainty is based on the uncertainty in all components of the calculation, while their uncertainty was based only on the uncertainty in the ΔN_2O/AOU ratio. The upper 60of our estimate overlaps with the lower 62of the **?** estimate. The biggest contributor to our this uncertainty is the f-ratio, especially in the tropics, which constitute 44% of the ocean surface area, and additional measurements and/or data-synthesis could help constrain the N_2O budget. The f-ratio data is only based on uptake of NO_3^-, NH_4^+ and urea, whereas phytoplankton can also take up NO_2^- and organic N (other than urea). One of the major sources of uncertainty in using the ΔN_2O/AOU ratio is that it is conceptually based on the N_2O production during nitrification, which uses O_2. N_2O production during denitrification is spatially separated from the associated O_2 use that is needed to nitrify the NO_3^-, the electron acceptor donor in denitrification. This NO_3^- is produced by nitrification, so in terms of mass balance our

calculation is still valid, but this N_2O production would show up as a vertical increase in N_2O without associated increase in AOU at low O_2 concentrations (high AOU) in Figure 4. This estimate of global marine N_2O production derived from analyzing the N cycle ~~(4.6 ± 3.1 Tg N y^{-1})~~ is statistically indistinguishable from the N_2O flux derived from ΔpN_2O observations~~(2.4 - 2.5 ± 0.8 Tg N y^{-1})~~, but has a much larger error. However, further observational constraints could not only reduce the error, but also ~~extend~~ further our understanding of the whole N cycle, including the option of evaluating ~~the model representation of these N cycle processes~~ their model representation against observations, and not just the part that N_2O plays in them. Such further constraints are also likely to provide the most productive way to reduce unexplained variability that is found in the observations but not in the present models. E.g., we have shown that both the N_2O and NO_3 are underestimated at ~300 - 1500 m depth and overestimated below ~2000 m (Fig. 6, 7). Thus, improved representation of mesopelagic remineralisation might lead in improved representation of the N_2O depth distribution. However, this falls outside the scope of this study.

Models of the global marine C cycle have been in use for decades, and a lot of the available information has been synthesized, cross-correlated and interpreted in detail (**??**). While actual measurements of N utilisation and transformation have also been made in abundance (Fig. 2, 3, 4, 5A, 6, 7, 9A), the synthesis and global modelling of these data is less advanced. In addition, N occurs in many different oxidation states in the marine environment (e.g. organic matter and NH_4^+ as -3, N_2 as 0, N_2O as 0 and +2, NO_2^- as +3, and NO_3^- as +5). Therefore, redox reactions complicate the representation of the N cycle a good deal. This lack of data synthesis and of identification of the most important controls in a complex system is reflected in a relatively low ability of the model to model observed nitrification rates and to a lesser extent NH_4^+ concentrations (Table 1).

This lack of knowledge also means that partitioning the global marine N_2O production over the nitrification and denitrification pathways is poorly constrained. Both the diagnostic and the prognostic models assign a small percentage of the total N_2O production to the denitrification pathway, 6 and 4% respectively. However, because of the large bias between the observed and modeled N_2O concentration depth profiles (Fig. 7) these may be underestimates (**??**). Possibly because of the model bias (Fig. 7, 8), the addition of N_2O consumption in the prognostic submodel does not lead to a significantly better distribution of N_2O across depth or between different basins (Fig. 8). As a result, the ΔpN_2O distributions are also quite similar (Fig. 10, 12) and the ~~optimised~~ optimized N_2O flux and confidence intervals of the two submodels are also quite similar (Fig. 11). However, it should also be noted, first, that the optimization using surface ΔpN_2O agrees with the optimization using N_2O concentration that the contribution of the low O_2 N_2O production needs to be low (Fig. 11). Second, the error contribution from the model vs. observed ΔpN_2O comparison is low, with confidence intervals of 0.3 Tg N y^{-1} for both submodels. Third, ΔpN_2O is equally well modelled above the low O_2 regions as in the rest of the ocean (Fig. 10, 12), and the contribution of the coastal and ~~near-shore non-coastal~~ deep offshore ocean are nearly proportional to their surface areas (Table 2). These three features are supporting evidence for our results that suggest that the low O_2 regions make a small contribution to the global ocean N_2O production. They should be balanced against the model bias of the vertical distribution of N_2O concentrations, which suggests a larger contribution from the low O_2 regions. **?** also estimated a small fraction of 7% of the global total contributed by denitrification / low O_2 N_2O production. Two complementary approaches could provide better constraints: a better representation of the vertical distribution of export and remineralisation would allow the optimization against N_2O concentration observations to achieve better results. But conversely, with better constraints on the physiology of nitrifiers and denitrifiers the

N_2O concentration database could provide constraints on the representation of remineralisation. Although there are relatively few N_2O concentration observations, nitrification and denitrification respond to specific environmental queues (in particular O_2 concentration), so that the they could contribute a relatively large observational constraint over the full range of environmental conditions.

Despite these shortcomings, the global marine N_2O flux is well constrained to 2.4 - 2.5 $\pm$ 0.8 Tg N y^{-1} by both submodels (Fig. 11). This ~~constraint~~ reflects the fact that the integrated effect of the different physical and biogeochemical processes determines the surface ΔpN_2O distribution (Fig. 10)~~, so that the integrated total can be well constrained even if the individual processes are not~~. The N_2O flux is at the lower end of previous estimates, and with a similar confidence interval to other recent estimates (Fig. 4). The confidence interval is dominated by uncertainty in the piston velocity (32%) rather than model-observation mismatches (12%). Because of differences in methodology it is not possible to provide reasons for why our estimate is lower than the more recent estimates. We can, however, compare our estimate to that of (**?**), because it is also based on a database of ΔpN_2O. Compared to their high end estimate using the piston velocity of Wanninkhof of 5.2 $\pm$ 3.6 Tg N y^{-1}, our estimate is lower because we use the more recent 13% lower estimate of piston velocity of (**?**), and because our ΔpN_2O of 7.6 $\pm$ 18.1 ppb is 25 - 28% lower compared to 10.55 natm in **?** (the range is calculated based on the water vapor correction for conversion between ppb and natm, which increases from 0.6 - 4.1% at temperatures from 0 - 30 °C, which brings the values slightly closer together).

We also tested how much influence sampling biases of very high supersaturation values might have on the estimated air-sea exchange. If the 40 ΔpN_2O measurements in the gridded database that are higher than 100 ppb (Fig. 12) are doubled, the ~~optimised~~ optimized N_2O air-sea exchange becomes 2.8 $\pm$ 0.5 Tg N y^{-1} for the diagnostic model and 3.1 $\pm$ 0.5 Tg N y^{-1} for the prognostic model. If the 24 ΔpN_2O measurements in the gridded database that are higher than 152 ppm are excluded, to decrease the frequency of the highly oversaturated observations down to what both submodels simulate (Fig. 12), the ~~optimised~~ optimized N_2O flux become 2.0 $\pm$ 0.2 for the diagnostic model and 2.3 $\pm$ 0.2 Tg N y^{-1} for the prognostic model. These results still fall within the confidence intervals of the results using the complete database.

Possible biases in ocean physical transport could in theory affect N_2O production in low O_2 regions. The indirect impact of ocean physics on low N_2O production through its impact on the distribution of O_2, which **?** have shown to be substantial, is not quantified here because we used observed O_2 (**?**) instead of modeled O_2. Our model results suggest that the model representation of ocean physics is adequate for the purpose of estimating N_2O flux from biogeochemical model perturbations. On the one hand, if the model had too much ventilation in the OMZs, shallow N_2O concentrations would be underestimated, as they are in the model (Fig. 7), but this would also lead to ΔpN_2O overestimation in the surface areas above the OMZs, which is not the case. The high ΔpN_2O are generally lower but spread over a larger area than in the observations (Fig. 10), with a good frequency distribution of high ΔpN_2O (Fig. 12). On the other hand, if the model had too little ventilation in the OMZs, the optimization would reduce N_2O production in the OMZs in compensation, but the optimization to ΔpN_2O would then estimate a higher OMZ N_2O production than the optimization to the N_2O depth profiles to compensate for the low transport, and this is also not the case. Therefore we conclude that potential biases in ocean physical transport do not appear to have a large direct impact on low N_2O production.

Possible biases in ocean physical transport could in theory affect N_2O production in low O_2 regions. However the model results do not suggest strong biases in N_2O production as a result. On the one hand, if the model had too much ventilation in the OMZs, shallow N_2O concentrations would be underestimated, as they are in the model (Fig. 7), but this would also lead to ΔpN_2O overestimation in the surface areas above the OMZs, which is not the case. The high ΔpN_2O are generally lower but spread over a larger area than in the observations (Fig. 10), with a good frequency distribution of high ΔpN_2O (Fig. 12). On the other hand, if the model had too little ventilation in the OMZs, the optimization would reduce N_2O production in the OMZs in compensation, but the optimization to ΔpN_2O would then estimate a higher OMZ N_2O production than the optimization to the N_2O depth profiles to compensate for the low transport, and this is also not the case. Therefore we conclude that potential biases in ocean physical transport do not appear to have a large direct impact on low N_2O production. The indirect impact of ocean physics on low N_2O production through its impact on the distribution of O_2, which **?** have shown to be substantial, is not quantified here because we used observed O_2 (**?**) instead of modeled O_2.

Global oceanic N_2O emissions estimated using atmospheric inversion methods based on atmospheric N_2O concentrations tend to be higher than our results (Fig. 4). However, N_2O emissions from inversions in the Southern Ocean are lower than the priors (**????**). These low Southern Ocean emissions (0.02 - 0.72 Tg N y^{-1}) are consistent with our results (0.68 - 0.79 Tg N y^{-1}). South of 30°S, 88% of the Earth surface is ocean, resulting in a clearer attribution in the inversions of the atmospheric N_2O anomalies to ocean fluxes. We suggest that the higher emissions estimates from inversions for the global ocean could be due to a combination of overestimated priors of ocean fluxes in combination with insufficient observational constraints at latitudes North of 30°S to allow correct partitioning between land and ocean fluxes. Results presented here are for the open and coastal ocean. The largest coastal seas are resolved in our model, although specific coastal processes, such as the interactions with sediments and tides, are not. Our results do not include emissions from estuaries. Fluxes from these could be as large as 2.3 - 3.6 Tg N y^{-1} according to one estimate (**?**), and could be another contributing factor to the difference between our results and those of atmospheric inversions.

Code and data availability. The four databases presented in this manuscript are available as NetCDF files from https://www.uea.ac.uk/green-ocean/data. The code of PlankTOM10.2 is available at greenocean-data.uea.ac.uk/model/PlankTOM10.2.tar

Competing interests. The authors declare they have no competing interests.

Acknowledgements. This research was supported by the European Commission's Horizon 2020 programme through the CRESCENDO and EMBRACE projects (projects 641816 and 282672). We thank Martin Johnson for the database of NH_4^+, and Andrew Yool for the database of nitrification rates. The MEMENTO database is administered by the Kiel Data Management Team at GEOMAR Helmholtz Centre for Ocean Research and supported by the German BMBF project SOPRAN (Surface Ocean Processes in the Anthropocene, http://sopran.pangaea.de).

We thank Alina Freing for providing the corrected numbers for the polynomial fit to the atmospheric pN2O data, and NOAA for providing atmospheric pN2O data.

Table 1. Cost function (Eq. 3) for the optimisation simulations of sections 2.2-2.4, relative to the respective observational databases. The nitrification rate in bold was used in this study.

Database	Model change	Cost function
Nitrication rate	0.2 d^{-1}	4.22
	0.1 $d^{-1} \times 2^{(T/10)}$	4.18
	0.79 $d^{-1} \times 2^{(T/10)} \times$ (1 - 0.159 $\times$ ln(O_2))	**4.16**
	0.58 $d^{-1} \times 2^{(T/10)} \times e^{(-0.14 \times I)}$	7.15
	4.7 $d^{-1} \times 2^{(T/10)} \times$ (1 - 0.159 $\times$ ln(O_2)) $\times e^{(-0.14 \times I)}$	6.87
Surface NH_4^+ concentration	$K_{1/2}$ estimated from observations	3.0

Table 2. Contributions of coastal (bottom depth $\leq$ 200 m), ~~near-shore non-coastal~~ deep offshore ($\leq 2^\circ$ from land, bottom depth > 200 m), East equatorial Pacific (180° - 70°W 5°S - 5°N, >2° from land) and rest of the open ocean (>2° from land, bottom depth > 200 m, excluding East Eq. Pac.) to N_2O flux, area and number of observations.

Region	Submodel	N_2O flux	% N_2O flux	% area	% n_{obs}
Coastal ocean	Diagnostic	0.05 $\pm$ 0.01	2	5	2
	Prognostic	0.041 $\pm$ 0.007	2		
Deep offshore	Diagnostic	0.33 $\pm$ 0.04	14	13	12
	Prognostic	0.37 $\pm$ 0.04	14		
East Eq. Pac.	Diagnostic	0.64 $\pm$ 0.05	27	22	17
	Prognostic	0.67 $\pm$ 0.05	25		
Open ocean	Diagnostic	1.37 $\pm$ 0.19	57	61	69
	Prognostic	1.54 $\pm$ 0.21	59		

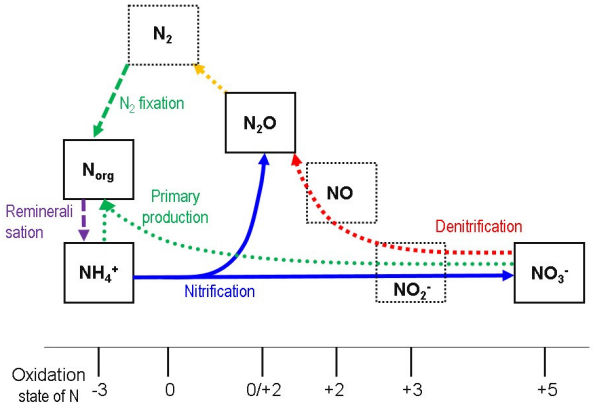

Figure 1. Primary biological pathways of the oceanic nitrogen cycle represented in the model simulations, along with redox states of N. Nitrification occurs in the oxic ocean (blue arrow). Denitrification yields net N_2O production in hypoxic conditions (red arrow) and net N_2O consumption in suboxic conditions (yellow arrow). Only organic nitrogen (N_{org}), NH_4^+, NO_3^- and N_2O are represented as model state variables.

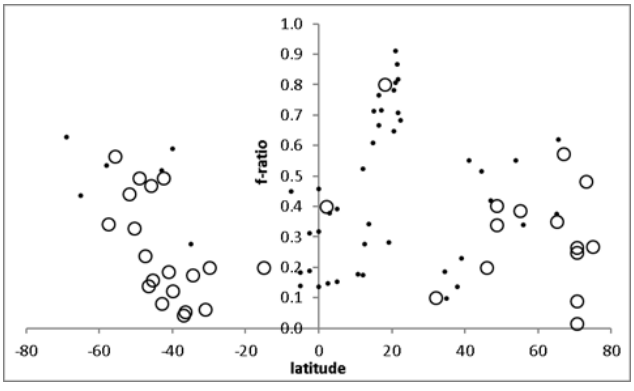

Figure 2. f-ratio ($\rho_{NO_3^-}/(\rho_{NO_3^-}+\rho_{NH_4^+}+\rho_{urea})$) as a function of latitude, from ^{15}N uptake experiments. Small dots were estimated without measuring NH_4^+ or urea concentrations (**????**). Large dots did not give a significant linear relationship with absolute value of latitude, and were therefore averaged at 0.29 ± 0.18 (**??????**).

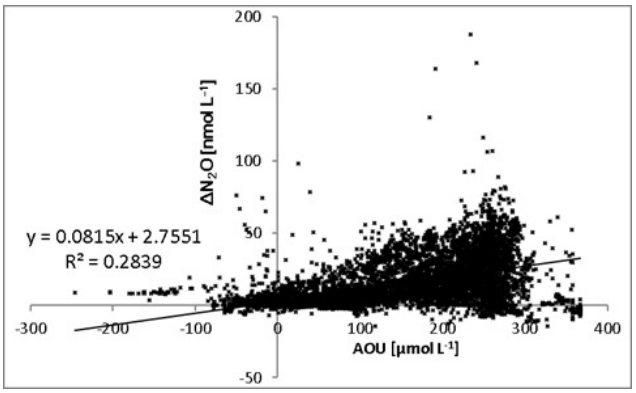

Figure 3. Apparent N_2O production (ΔN_2O nmol L^{-1}) as a function of apparent oxygen utilization (AOU μmol L^{-1}).

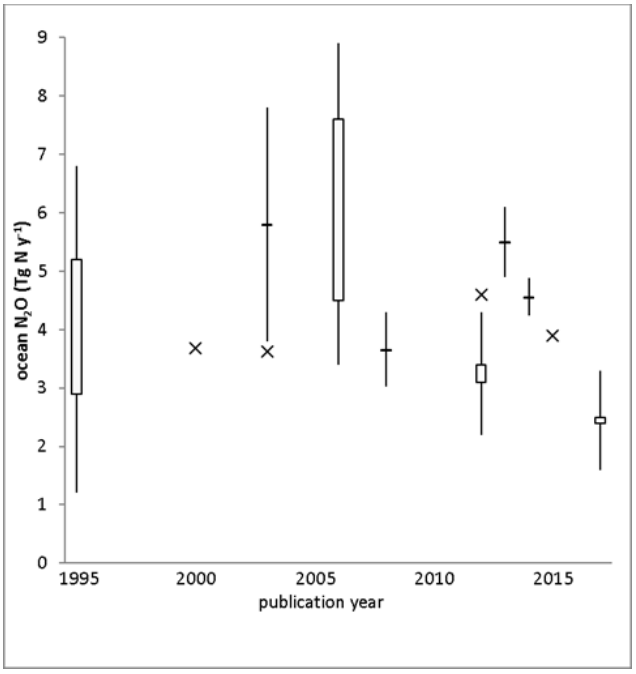

Figure 4. Published estimates of global ocean N_2O production or air-sea exchange. Estimates based on global observational datasets shown as boxes when ranges are given and whiskers if error estimates are given (ocean observations: **???** (plotted in 2011), **?**, this study; atmospheric inversions: **???** (plotted in 2013), **?**), model estimates shown as crosses (**????**).

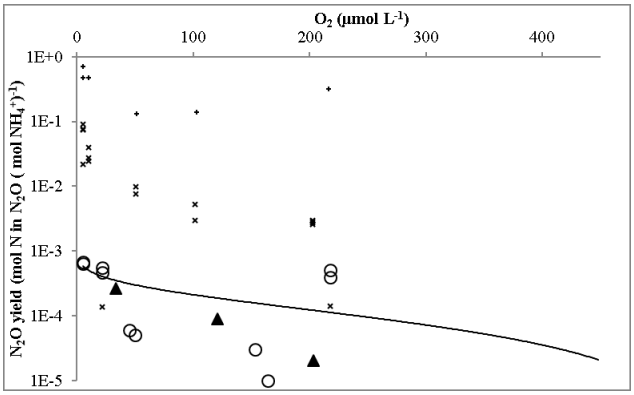

Figure 5. N_2O yield of nitrification (N atom:atom) as a function of O_2 concentration, filled triangles: AOA (**?**), open circles: AOB at low to medium cell numbers (**??**), crosses: marine AOB at high cell numbers (**??**), plusses: soil AOB at high cell numbers (**?**). Black line: logarithmic fit to AOA and low to medium cell number AOB (yield = 0.791-0.126·ln(O_2) mmol N in N_2O (mol NH_4^+)$^{-1}$).

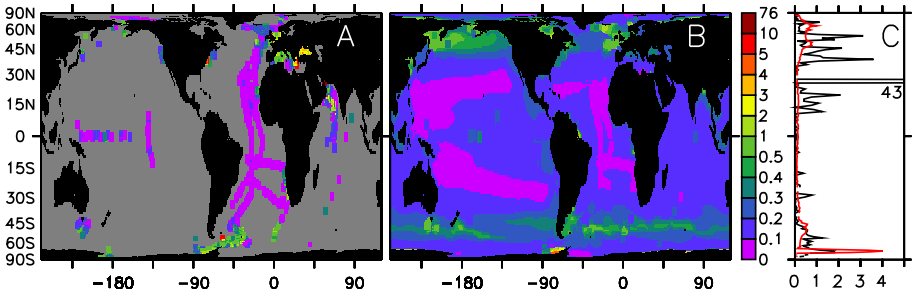

Figure 6. Surface NH_4^+ concentration (μmol L^{-1}). A) observations~~(symbol size is 5 × 5°)~~. B) model results are for the same months where there are observations, and annual averages everywhere else. C) zonal average, black) observations, red) model results. Model results are for the same months and longitudes as the observations. Latitude y-axis to the left of panel A.

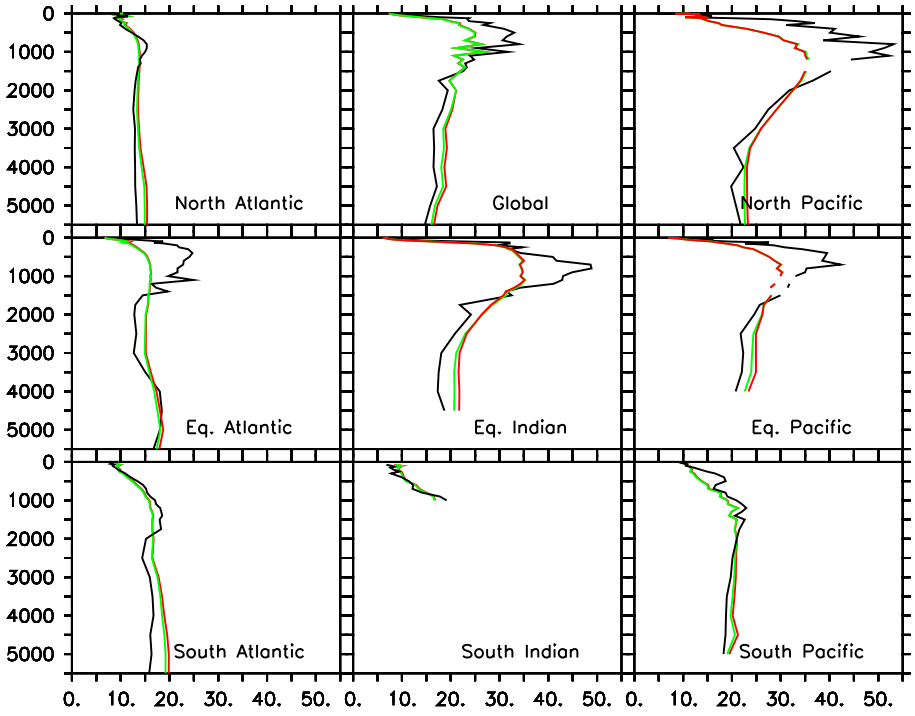

Figure 7. Depth profiles of N_2O concentration (nmol L^{-1}) for different basins. Black lines: observations, Green lines: optimised diagnostic model, Red lines: optimised prognostic model.

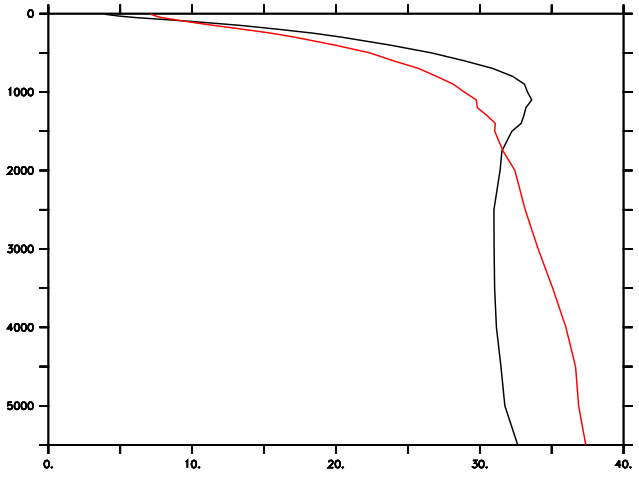

Figure 8. Depth (m.) profile of average NO_3^- concentration (μmol L^{-1}). Black line) WOA2009 synthesis of observations, not interpolated. Red line) Model results sampled at the places where there are observations.

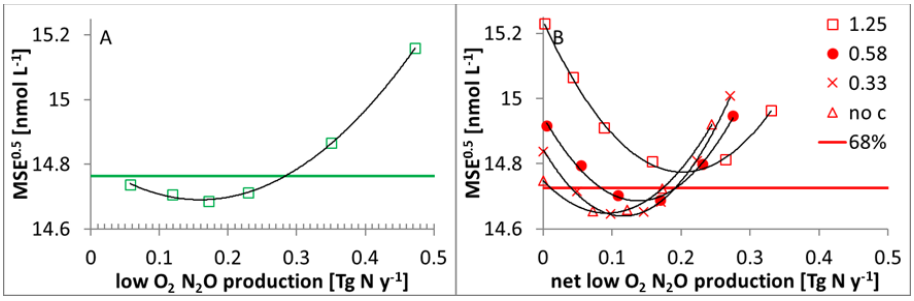

Figure 9. $MSE^{0.5}$ for the two N_2O submodels compared to the N_2O concentration database as a function N_2O production in the low O_2 regions. MSE_{min} was obtained as the minimum of a second order polynomial fit (black lines). The 1σ confidence interval, where MSE equals the value calculated from Eq. 5, is indicated by the horizontal lines. A) diagnostic submodel, each point represents a simulation with a different low O_2 ratio, B) prognostic model, "no c" is with no N_2O consumption i.e. net production = gross production. All other lines have a constant gross production, and net production varies with different N_2O consumption rates. Range of parameter values is given in the supplementary material Section 8.7.

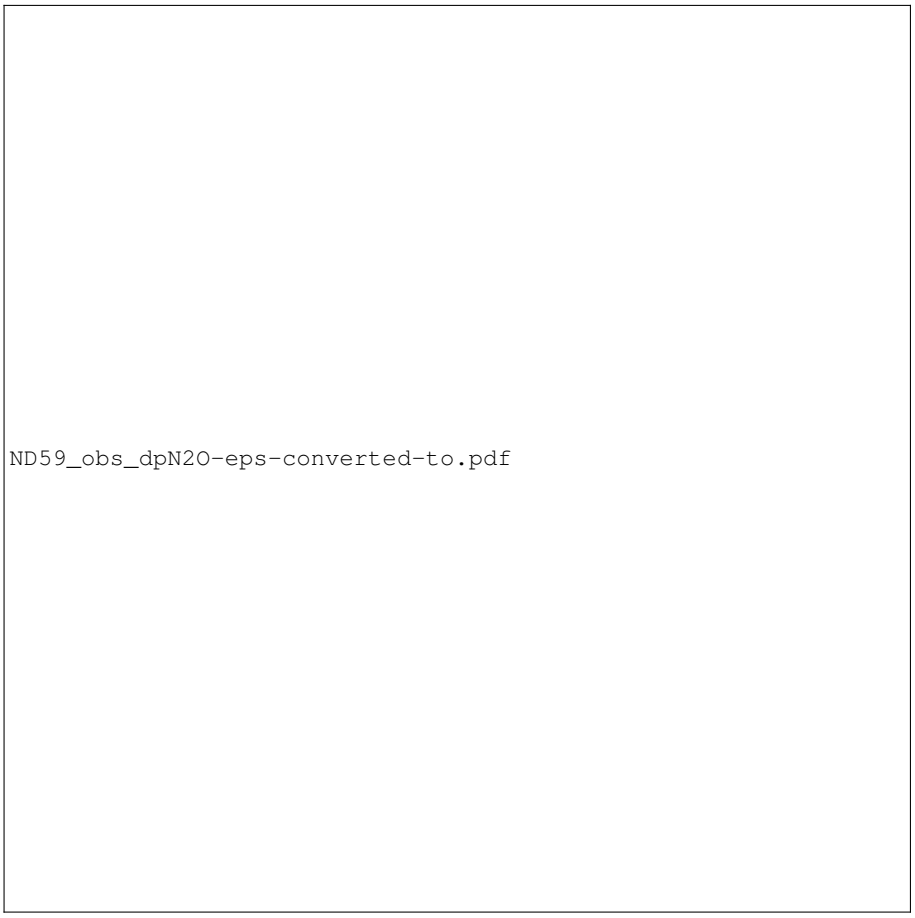

Figure 10. Surface ΔpN_2O (ppb). A) observations~~(symbol size is 5 × 5°)~~, B) optimised diagnostic model, C) optimised prognostic model. Model results are for the same months where there are observations, and annual averages everywhere else. D) zonal average, Black line: observations, Green dashed: diagnostic model, Red dotted: prognostic model. Model results are for the same months and longitudes as the observations. Latitude y-axis to the left of panel A.

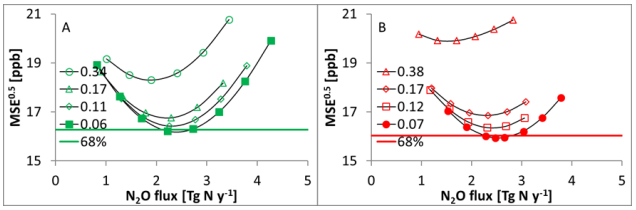

Figure 11. $MSE^{0.5}$ for the two N_2O submodels compared to the ΔpN_2O database as a function of global N_2O flux at different (net) N_2O production rates in the low O_2 regions. MSE_{min} and confidence intervals as in Fig. 8. A) diagnostic submodel, the four lines represent the four best low O_2 production rates from Fig. 9A, each point represents a simulation, different symbols indicate different low O_2 ratios, points with the same symbols have different oxic N_2O production ratios. B) prognostic submodel, the four lines represent the optimised net production rates at the four best gross production rates from Fig 9B, points with the same symbols have different N_2O ratios for nitrification.

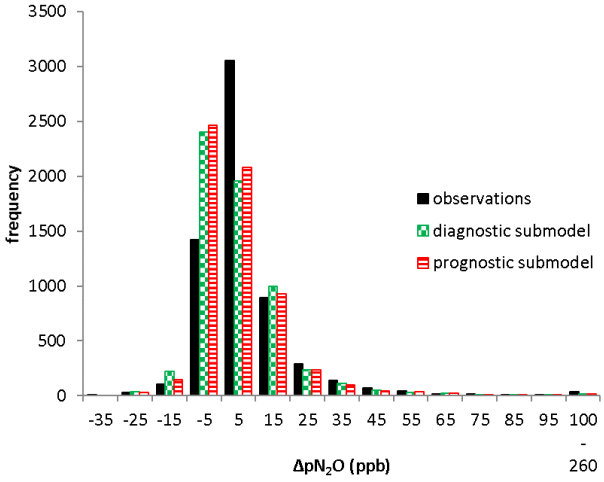

Figure 12. Frequency distribution of ΔpN_2O in the observations (solid black), and the optimised simulations of the diagnostic submodel (green squares) and the prognostic submodel (red lines).